AGU
ADVANCING EARTH AND SPACE SCIENCE

Geophysical Research Letters

Soil Organic Carbon Development and Turnover in Natural and Disturbed Salt Marsh Environments

Sheron Y. Luk[1,2] 📖, Katherine Todd-Brown[3] 📖, Meagan Eagle[4] 📖, Ann P. McNichol[5] 📖, Jonathan Sanderman[6] 📖, Kelsey Gosselin[2] 📖, and Amanda C. Spivak[7] 📖

[1]Massachusetts Institute of Technology - Woods Hole Oceanographic Institution Joint Program in Oceanography and Applied Ocean Science and Engineering, Cambridge, MA, USA, [2]Marine Chemistry and Geochemistry Department, Woods Hole Oceanographic Institution, Woods Hole, MA, USA, [3]Department of Environmental Engineering Sciences, University of Florida, Gainesville, FL, USA, [4]Woods Hole Coastal and Marine Science Center, U.S. Geological Survey, Woods Hole, MA, USA, [5]Marine Geology and Geophysics Department, Woods Hole Oceanographic Institution, Woods Hole, MA, USA, [6]Woods Hole Research Center, Falmouth, MA, USA, [7]Department of Marine Sciences, University of Georgia, Athens, GA, USA

Abstract Salt marsh survival with sea-level rise (SLR) increasingly relies on soil organic carbon (SOC) accumulation and preservation. Using a novel combination of geochemical approaches, we characterized fine SOC (≤1 mm) supporting marsh elevation maintenance. Overlaying thermal reactivity, source (δ^{13}C), and age (F^{14}C) information demonstrates several processes contributing to soil development: marsh grass production, redeposition of eroded material, and microbial reworking. Redeposition of old carbon, likely from creekbanks, represented ~9%–17% of shallow SOC (≤26 cm). Soils stored marsh grass-derived compounds with a range of reactivities that were reworked over centuries-to-millennia. Decomposition decreases SOC thermal reactivity throughout the soil column while the decades-long disturbance of ponding accelerated this shift in surface horizons. Empirically derived estimates of SOC turnover based on geochemical composition spanned a wide range (640–9,951 years) and have the potential to inform predictions of marsh ecosystem evolution.

Plain Language Summary Salt marsh survival with rising sea levels increasingly depends on the accumulation and preservation of buried organic carbon. Marsh soil organic carbon development reflects at least three processes: burial of differently reactive compounds that derive from local grasses, redeposition of old carbon (9%–17%), and microbial reworking. Decomposition results in a progressive decrease in the thermal reactivity of soil organic carbon, and disturbances such as ponding can accelerate this shift. Modeled rates of geochemically defined soil organic carbon pools turnover on the order of centuries-to-millennia and can refine predictions of salt marsh sustainability.

1. Introduction

Salt marshes maintain elevation in the tidal frame through rapid vertical accretion supported by efficient burial of minerals and organic matter. Soil accumulation and preservation support valuable ecosystem services (Barbier et al., 2011) and are critical to salt marsh survival as sea-level rise (SLR; Morris et al., 2002, 2016). Declining mineral inputs to certain marshes (Weston, 2014) place additional importance on soil organic carbon (SOC) preservation. Global climate change-induced disturbances are expected to increase SOC vulnerability to decomposition, potentially leading to marsh subsidence (Pendleton et al., 2012; Spivak et al., 2019). Characterizing SOC composition and reactivity and how those properties are changed by decomposition is key to predicting future marsh sustainability and carbon storage.

Efficient SOC burial and preservation largely reflect high rates of primary production and slow decomposition. Under anoxic conditions of marsh soils, decomposition is often conceptualized as modified decay functions with labile and refractory compounds turning over on time scales of months-to-years and centuries-to-millennia, respectively (Kirwan & Mudd, 2012). Slow-cycling SOC is the critical component supporting carbon storage and elevation maintenance. It is often estimated at 10%–20% of annual organic matter production and composed of macromolecules such as lignin (Kirwan & Mudd, 2012; Morris & Bowden, 1986; Schile et al., 2014). Recent evidence that environmental constraints on microbial communities limit decomposition rather than intrinsic molecular recalcitrance (Lehmann et al., 2020; Marín-Spiotta

et al., 2014) suggests that marsh soils likely preserve a broad mixture of compounds with differing reactivities. Assessing how decomposition changes the composition and reactivity of slow-cycling SOC can provide insight into controls on preservation as well as potential for loss following disturbances.

Rapid SLR and certain hydrological management practices have contributed to the expansion of shallow ponds in many salt marshes (Adamowicz & Roman, 2005; Watson et al., 2017). While permanently inundated ponds are natural features that can exist for decades before draining and recovering (Mariotti et al., 2020), runaway expansion has been described as a transitional state between healthy and drowning marshes (Kirwan & Murray, 2007; Ortiz et al., 2017). Ponds typically form following disturbances that cause marsh vegetation dieback (e.g., waterlogging) and deepen through decomposition of underlying peat (Johnston et al., 2003; Spivak et al., 2018). Ponds therefore offer a natural, decadal-scale experiment for evaluating how disturbances that accelerate decomposition alter slow-cycling SOC.

We assessed how slow-cycling SOC composition and reactivity changes over decades-to-millennia and in response to the disturbance of ponding in a temperate salt marsh. We hypothesized that marshes bury a range of compounds with differing reactivities that derive from local production but long-term decomposition results in a progressive homogenization and decrease in SOC reactivity. Further, we predicted that the disturbance of ponding accelerates decomposition-driven changes in SOC composition and reactivity. SOC reactivity, sources, and age were characterized by overlaying thermal properties and isotopic composition (δ^{13}C, F^{14}C). We estimated the turnover times of slow-cycling SOC by modeling changes in composition against geochronologies developed from radioisotope-based age models and SLR reconstructions.

2. Methods

2.1. Study Sites

We collected soil cores from three sites within the Plum Island Ecosystems – Long Term Ecological Research (PIE-LTER) domain (MA, USA; 42.74°N, −70.85°W; Figure S1). The sites are within marshes that formed prior to European settlement (Kirwan et al., 2011) and had similar elevations (1.41–1.51 m North American Vertical Datum of 1988 [NAVD88]) and high marsh plant communities, dominated by *Spartina alterniflora*, *S. patens*, and *Distichlis spicata*, that are typical of New England marshes (Redfield, 1972). Permanently inundated ponds within each site had comparable depths (0.24–0.30 m) but varied in size (643–7,149 m^2) and age (40–53 years; Spivak et al., 2017, 2018). Paired soil cores were collected from the marsh platform (100 cm) and a pond (50 cm) within each site; differences in core length reflected lower surface elevations in the ponds relative to the marsh.

2.2. Bulk Soil Properties

Soil cores were sectioned at 1, 2, or 5 cm intervals, with higher resolution in the top 30 cm (supporting information 2.1). Soil water content (%) and bulk density (g cm^{-3}) were determined gravimetrically. Samples were sieved (1 mm) to remove large roots. We focused on particles (≤1 mm) passed through the sieve that are consistent with functional definitions of slow-cycling fine SOC (Bruun et al., 2010; Hemminga et al., 1988; Williams & Rosenheim, 2015). Samples were ball milled and ∼90% were fumed with hydrochloric acid and analyzed for bulk elemental (total organic carbon [TOC (%, kg m^{-3})]) and isotopic (δ^{13}C, ‰) composition. Carbon content of the remaining 10% was estimated from a diffuse reflectance Fourier Transform Mid-infrared spectroscopy partial least squares regression model (supporting information 2.2; Janik et al., 2007).

2.3. Bulk Soil Data Analysis

We compared bulk soil and elemental properties across three depths: (i) shallow marsh rooting zone (0–30 cm), (ii) intermediate marsh horizons (30–54 cm) that overlapped with pond surface horizons (0–24 cm), and (iii) deep marsh (54–77 cm) and pond (24–50 cm) horizons. Means and standard errors (SE) of soil properties were calculated in 6 cm increments (supporting information 2.3). Marsh and pond cores across the three sites were used as independent replicates to conduct one-way analysis of variance tests, which

were used to detect differences within the three depth zones of marsh and pond soils separately, and between marsh and pond downcore profiles at corresponding 6 cm increments based on elevation.

2.4. Thermal Reactivity and Carbon Isotope Measurements

SOC thermal properties and reactivity indices were characterized through ramped pyrolysis oxidation (RPO) for horizons representing key parts of the soil profiles, including the marsh and pond surface, base of the marsh rooting zone, and deeper horizons representing carbon buried for more than 100 years. Homogenized samples (~6 mg) were heated to 1,000°C at a rate of 20°C min^{-1} (Rosenheim et al., 2008) and the evolved carbon dioxide (CO_2) was measured by a flow-through infrared gas analyzer. Thermograms were constructed by plotting CO_2 concentrations versus temperature (supporting information 2.5). Samples were not acidified as inorganic carbon content was <0.04% of TOC. Analyses were conducted at the National Ocean Sciences Accelerator Mass Spectrometry Facility (MA, USA).

We further analyzed CO_2 evolved via RPO for $\delta^{13}C$ and $F^{14}C$ composition (McNichol et al., 1994; Reimer et al., 2004) from one representative marsh and pond site (supporting information 2.4). The CO_2 fractions were collected over five temperature intervals; there were three low (200°C–465°C) and two high (465°C–650°C) temperature CO_2 fractions. The isotopic composition of evolved CO_2 was analyzed for at least three of the five fractions, capturing ~70% of TOC within a soil horizon.

2.5. Thermal Reactivity and Isotope Data Analysis

We evaluated SOC thermal reactivity within and between marsh and pond environments by calculating ratios of CO_2 evolved at low versus high temperatures (hereafter, peak ratio) and thermal activation energies (supporting information 2.5). Peak ratios were determined by normalizing the area under the low (200°C–465°C) versus high (465°C–650°C) temperature peaks of the thermograms. The theoretical activation energy (*Ea* kJ mol^{-1}) and blank contamination correction were calculated using the Python package *rampedpyrox* (Hemingway et al., 2017a, 2017b). The mean and SE of peak ratios and *Ea* were calculated across 25 cm increments based on elevation.

2.6. Age Models

Soil horizon ages across all sites were constrained with several inputs in order to conservatively model turnover times. Post-1900 accretion rates were calculated using ^{210}Pb constant initial concentration (CIC) and continuous rate of supply (CRS) models with radioisotope activities measured on planar-type gamma counters (Canberra Inc., USA). Contemporary rates of SLR, from a local tide gauge (Boston 8443870, 2.83 ± 0.15 mm year^{-1}), provided an age constraint for the past century based on the assumption that the marsh kept pace with SLR (Appleby & Oldfield, 1978; Pennington et al., 1976). For pre-1900 horizons, we extended CIC-^{210}Pb-based accretion rates deeper in the soil profile, while upper age limits were constrained with late-Holocene SLR (0.6 ± 0.1 mm year^{-1} and 0.9 ± 0.2 mm year^{-1}; Engelhart et al., 2009; Gonneea et al., 2019), and glacial isostatic adjustment (1.2 mm year^{-1}; Peltier et al., 2015). Age models were not developed for the ponds due to the violation of steady-state assumptions as ^{210}Pb inventories suggested erosion (supporting information 2.6).

2.7. Soil Turnover Models

We estimated turnover times of fine SOC in the marsh platform using a depth-for-time substitution where downcore changes in carbon concentration were modeled against geochronology. First, across all marsh sites, a one-pool model captured changes in total fine SOC concentrations and a two-pool model was developed from persistent low-temperature and high-temperature thermogram peaks. We expanded to a five-pool model based on thermal and isotopic data at one site suggesting at least five compositionally distinct SOC

pools. For the two-pool and five-pool models, carbon concentrations within each consecutive pool were defined as the amount of CO_2 evolved over discrete increasing temperature intervals within the thermogram.

$$U_i(t) = U_{\text{initial,i}} - \frac{U_{\text{initial,i}}}{t_{\text{root}}} \times t \quad \text{if } t < t_{\text{root}} \tag{1}$$

$$\text{for } i = 1 : \frac{\mathrm{d}x_i(t)}{\mathrm{d}t} = U_i(t) - \frac{1}{\tau_i} \times x_i(t) \tag{2}$$

$$\text{for } i > 1 : \quad \frac{\mathrm{d}x_i(t)}{\mathrm{d}t} = U_i(t) + (r_{i-1}) \times \frac{1}{\tau_{i-1}} \times x_{i-1}(t) - \frac{1}{\tau_i} \times x_i(t) \tag{3}$$

Turnover in the first pool ($i = 1$) is described as first-order kinetics dictated by the carbon concentration of the pool (x) at a given time obtained from the age models (t), linear input (U) during the time within the rooting zone (t_{root}), and turnover time (τ; Equations 1 and 2; Manzoni et al., 2009). Subsequent pools ($i > 1$) are a linear series, where a fraction (r_{i-1}) of decomposed material from the previous pool is transferred to the next pool (Equation 3). For further details on SOC turnover model parameterization, see supporting information 2.7.

3. Results

3.1. Bulk Soil Properties

Bulk soil properties changed with depth and differed between the marsh and ponds. In the marsh, water and TOC content (% and kg m^{-3}) decreased while bulk density increased with depth (Figure 1). Pond soil properties were less variable across depths, with the exception of TOC (%) which decreased slightly. Marsh soils were generally drier and had higher bulk densities than the ponds (Figures 1a and 1b, Table S1). Marsh and pond soils had similar TOC densities (kg m^{-3}), except in pond surface horizons where lower concentrations reflected lower bulk densities (Figure 1d, Table S1). Bulk TOC content informed the one-pool turnover model.

3.2. SOC Reactivity

There was a bimodal distribution of CO_2 evolved during RPO with low ($371°C \pm 4°C$) and high ($530°C \pm 4°C$) temperature peaks separated by a minimum at $465.5°C \pm 2.4°C$ (Figures 2a–2g). Peak ratios decreased while *Ea* increased with depth in marsh soils (Figures 2h and 2i), indicating a shift toward lower thermal reactivity. Pond surface horizons had lower peak ratios and higher *Ea* values than the marsh (~1.2 m NAVD88), but the reactivity indices converged toward similar values in both environments at ~1 m elevation (Figures 2h and 2i, Table S2). The bimodal thermogram distribution across soil depths suggests the presence of at least two distinct fine SOC pools and was the basis of the two-pool turnover model.

3.3. SOC Sources and Ages

The $\delta^{13}C$-CO_2 values associated with different temperature intervals spanned a wider range than bulk SOC (Figure 3). The $\delta^{13}C$-CO_2 of the low-temperature peak ($-15.5 \pm 0.2‰$) was similar to bulk soils ($-15.0 \pm 0.3‰$), while the high-temperature peak was more enriched ($-13.8 \pm 0.2‰$). These data are consistent with emergent grasses as the main carbon source to marsh and pond soils (Spivak & Ossolinski, 2016) with variation between peaks suggesting differences in molecular composition (Benner et al., 1987).

Radiocarbon ($F^{14}C$) values were highest in CO_2 fractions evolved at lower temperatures, reflecting more modern inputs, and decreased with higher temperatures (Figure 3, Table S5). This trend was clearest within the marsh (0–26 cm) and pond surface horizons (0–2 cm), where modern values were expected. These data indicate that old, marsh derived, and thermally stable carbon represent substantial components (9%–17%)
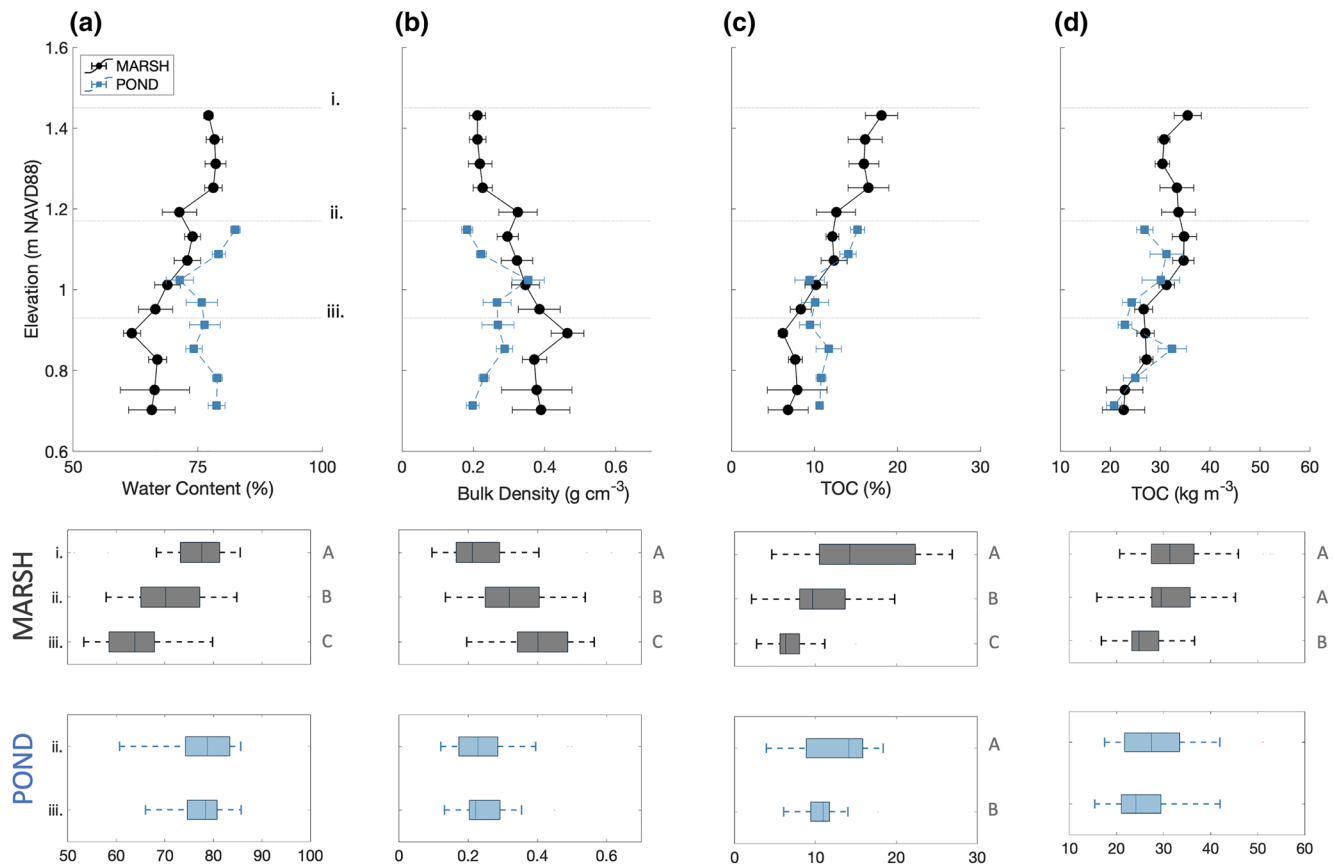
Figure 1. (Top) Marsh and pond soil (a) water content, (b) bulk density, and (c and d) TOC content at 6 cm increments and (bottom) within pooled depth zones: (i) shallow marsh (0–30 cm), (ii) intermediate marsh (30–54 cm) and shallow pond (0–24 cm), and (iii) deep marsh (54–77 cm) and pond (24–50 cm). Data represent means and SE; uppercase letters indicate zones are significantly different ($p < 0.05$) within marsh and pond soils, separately (supporting information 2.3). TOC, total organic carbon; SE, standard error.

of shallow horizons. Overlaid thermal reactivity, source, and age data point to at least five compositionally distinct fine SOC pools and were the basis of the five-pool turnover model.

3.4. Soil Age Models

Mean soil accretion rates from the CRS and CIC models for contemporary (post-1900s) deposition were 4.64 ± 0.38 mm year^{-1} and 2.47 ± 0.39 mm year^{-1}, respectively (Luk et al., 2020; Table S3). Horizons deeper than 28 cm reached the limitation of ^{210}Pb dating (pre-1900s). Conservative age estimates for the deepest horizon (80 cm) ranged from 219 years to 1,194 years (Table S4).

3.5. Marsh SOC Turnover Models

The one-pool model, based on TOC content, yielded a best fit turnover time of 750 years (Figure 4a). This was similar to rates calculated from the two-pool model, which was based on the low-temperature and high-temperature peaks in the RPO thermograms (640 and 1,251, respectively; Figure 4b, Table S6). The five-pool model, based on geochemical composition (Figure 3), captured a broader distribution of turnover times, ranging from 1,011 years to 9,951 years, with generally faster rates for the first and second pools (Figure 4c, Table S6). Fitting one-pool and two-pool models across the three marsh sites resulted in similar goodness-of-fit statistics, which were higher than the five-pool model at the one marsh site; this was due, in part, to lower data densities (Table S6). These results highlight the continuum of fine SOC turnover times.
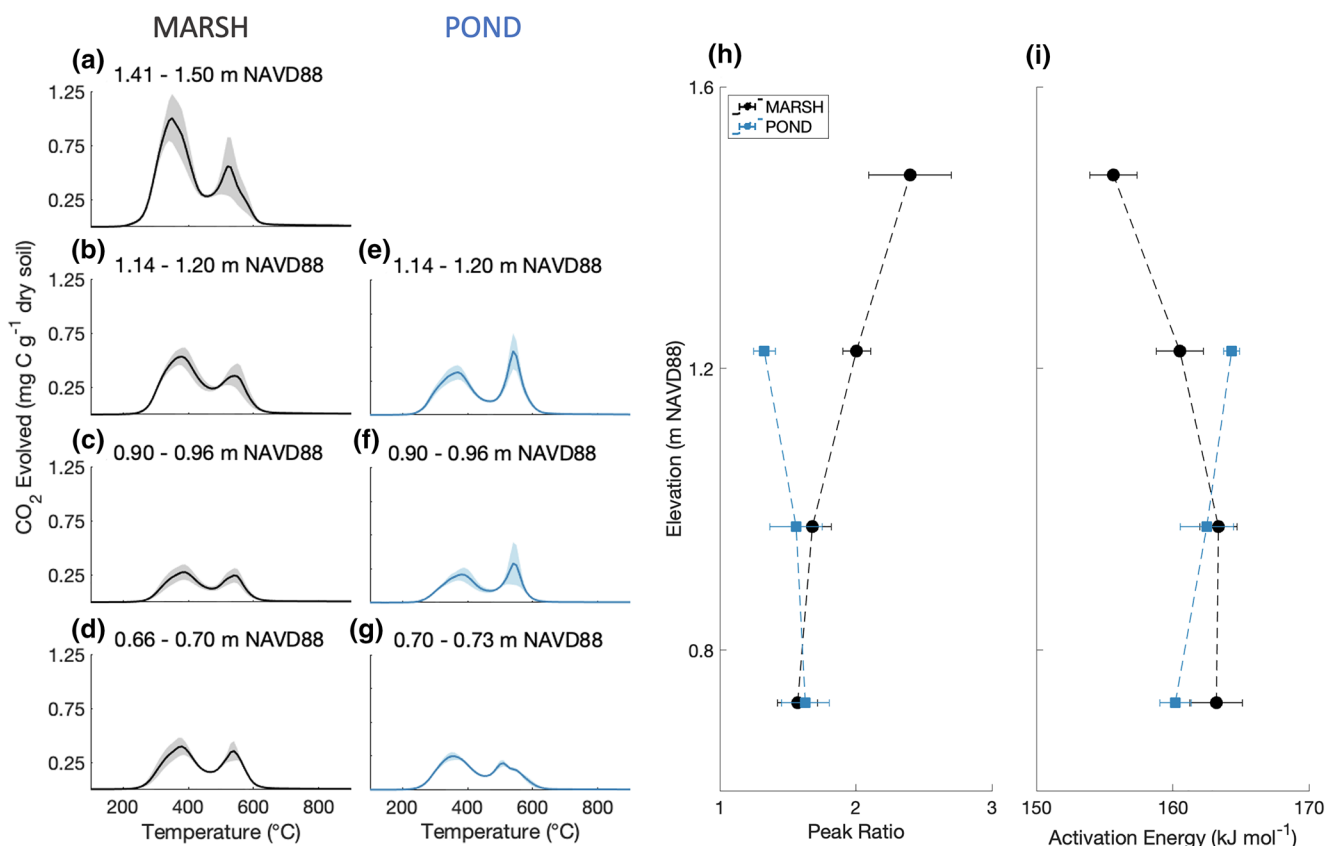
Figure 2. Thermograms of the mean and SE of CO_2 evolved from marsh and pond horizons at similar elevations (a–g) were used to calculate two thermal reactivity indices, low-temperature versus high-temperature peak ratios (h) and activation energy required to combust SOC (i) (supporting information 2.5). SE, standard error; SOC, soil organic carbon.

4. Discussion

4.1. SOC Composition

Soils in this New England salt marsh buried compounds with a range of thermal properties and $\delta^{13}C$ values indicating that they derived from marsh grasses (Figures 2 and 3; Spivak & Ossolinski, 2016). The wider range of $\delta^{13}C$-CO_2 measured across the thermograms, compared to bulk soils, likely reflects differences in the isotopic composition of compounds synthesized by marsh grasses (Figure 3). For instance, *S. alterniflora* is rich in cellulose and hemicellulose (~70%, −11.5‰) with lower levels of lignin (4%–9%, −17.4‰) and other compounds, such as lipids, carbohydrates, and amino acids (~22%, −16.2‰; Figures 2 and 3; Benner et al., 1987). Compounds in this latter group are likely decomposed rapidly, with contributions attenuating with depth. The $\delta^{13}C$-CO_2 values suggest that there was not a clear separation between compound classes across temperature intervals, potentially reflecting overlapping thermal properties as well as microbial re-working and aggregate formation (Figure 3; Bruun et al., 2010). Work in terrestrial soils consistently shows an enrichment in $\delta^{13}C$ of 2‰–4‰ along gradients of increasing decomposition (Sollins et al., 2006) and thermal stability (Sanderman & Grandy, 2020). It is unlikely that measured $\delta^{13}C$-CO_2 values are methodological artifacts, as they spanned a greater range than predicted by kinetic fractionation and enrichment did not increase monotonically with temperature (Figure 3; Hemingway et al., 2017b). This result highlights that thermal properties provide an index of reactivity that may not reflect bioavailability, which depends on environmental conditions, among other factors (Bulseco et al., 2019, 2020; Lehmann et al., 2020).

Although salt marshes are efficient carbon sinks, SOC stocks are spatially heterogeneous (Ouyang & Lee, 2014). Compared to this New England marsh, thermogram complexity, TOC%, and Ea were lower in a Gulf of Mexico marsh with similar grass communities (Williams & Rosenheim, 2015). Factors contributing
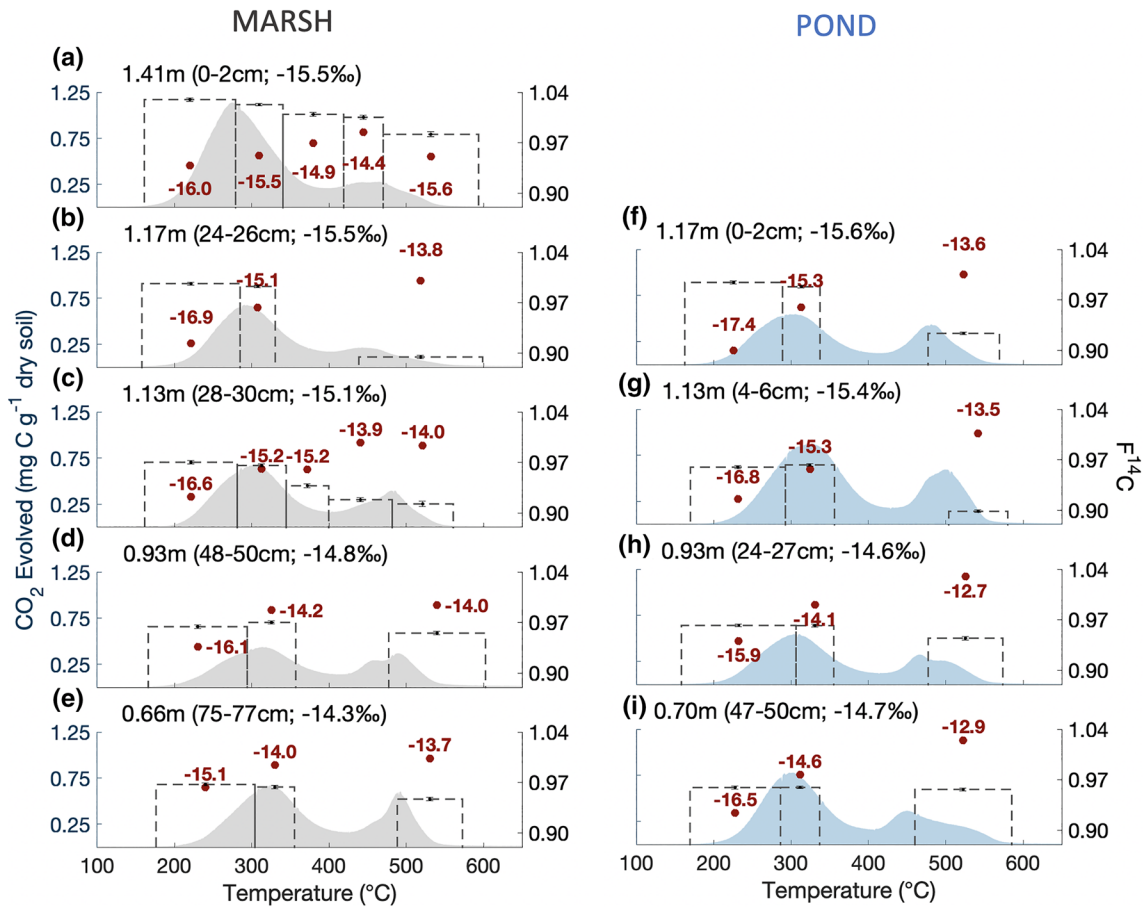
Figure 3. Thermal properties, sources (δ^{13}C), and ages (F^{14}C) of marsh (a–e) and pond (f–i) SOC at one site. Dotted bars are F^{14}C values for CO_2 fractions collected over a temperature interval (bar width) with associated analytical error. The δ^{13}C-CO_2 from fractions are indicated in red. Pond and marsh horizons were paired by elevation (NAVD88, m); soil depth and bulk soil δ^{13}C are in parentheses (supporting information 2.4). NAVD88, North American Vertical Datum of 1988.
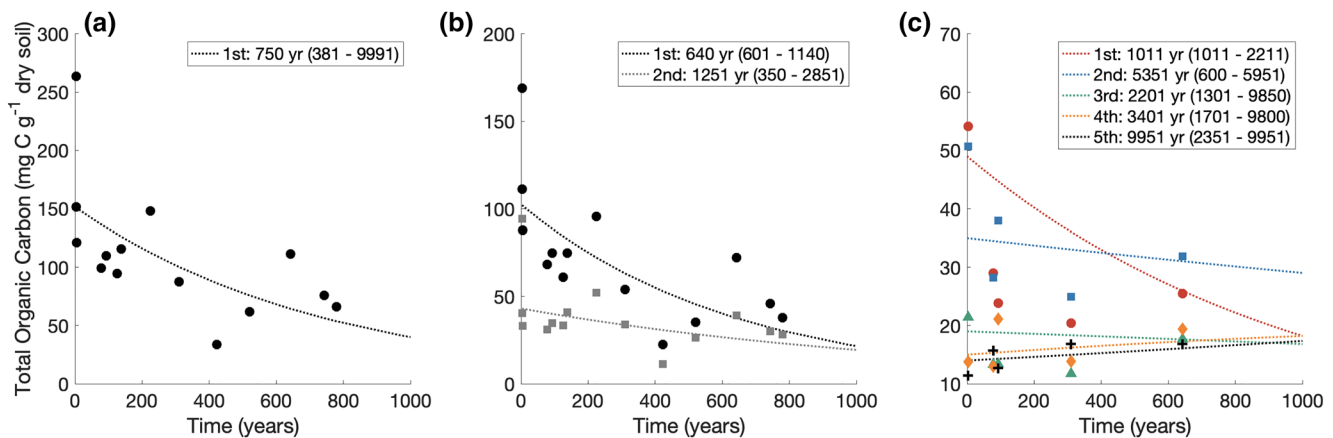
Figure 4. Turnover times estimated by (a) one-pool and (b) two-pool models for all marsh sites and (c) a five-pool model for one marsh site. Measured CO_2 concentrations (dots) from compositionally distinct fine SOC CO_2 fractions were modeled against soil age estimates in years. Dashed lines are modeled turnover times. Inset lists the best fit rate and range for each modeled pool (Table S6; supporting information 2.7). SOC, soil organic carbon.

to these differences are unclear but applying thermal and isotopic characterization approaches more broadly may provide insight into controls on marsh SOC preservation (Lehmann et al., 2020).

The $F^{14}C$ values within and across depth horizons reveal multiple processes contributing to marsh soil development (Figures 3a–3e). In shallow horizons (0–26 cm), new production was an important component of lower temperature CO_2 fractions while $F^{14}C$ values of <1 at higher temperatures suggest either redeposition of eroded creekbank carbon or microbial recycling (Figures 3a and 3b). The effects of microbial reworking on $F^{14}C$ are likely minor in surface horizons, due to rapid vertical accretion (Table S3). This relatively old, thermally stable fraction represents ∼9% of surface (0–2 cm) and 17% of deeper (24–26 cm) SOC, which is consistent with previous estimates based on creekbank erosion in this system (Figures 3a and 3b; Hopkinson et al., 2018). Since redistribution of previously buried soils contributes to accretion, current SOC storage estimates are likely upwardly biased. Redeposition of eroded soils may become increasingly important in maintaining marsh elevation with SLR (Hughes et al., 2009) and accounting for spatial recycling of carbon will be key for refining carbon budgets.

4.2. SOC Turnover Under Natural Conditions

Marsh soil profiles are consistent with long-term alteration due to decomposition, rather than changes in autochthonous versus allochthonous inputs. Increasing bulk densities and decreasing water and TOC content below the rooting zone (0–28 cm) suggest loss of organic matter, compaction, and dewatering (Figure 1). Decreasing thermal reactivity with depth (Figures 2h and 2i) coincided with a small $\delta^{13}C$-CO_2 enrichment across CO_2 fractions (Figures 3a–3e). It is difficult to ascertain whether the preferential loss of specific compounds (i.e., Benner et al., 1987) or microbial reworking and development of microbial derived residues contributes to $\delta^{13}C$-CO_2 enrichment and homogenization of $F^{14}C$ values with increasing soil depth (Figure 3, Gleixner et al., 2002; Trumbore, 1997, 2009). Transitions in dominant vegetation associated with ecosystem evolution (Kirwan et al., 2011) would have a small effect on our results since *S. alterniflora*, *S. patens*, and *D. spicata* have similar biochemical compositions (Cristina et al., 2018; Haddad & Martens, 1987; Wilson et al., 1986). Thus, the anoxic environment of marsh soils enhances preservation but does not completely inhibit microbial alteration of SOC.

Quantifying SOC loss alongside geochronometers can constrain turnover times that are difficult to measure experimentally. The best fit rates from the one-pool, two-pool, and five-pool models span a broader range (640–9,951 years; Figure 4, Table S6) than applied by some marsh evolution models (200–1,000 years; Day et al., 1999; Kirwan & Mudd, 2012). Our one-pool model describes continuous loss of SOC, while the five-pool model predicts accumulation of the more thermally stable SOC, due to slower turnover and increased transfer (r_{i-1}) over time (Figure 4, Table S6). The five-pool model therefore describes important mechanisms contributing to SOC preservation and marsh elevation gain that are not captured by the one-pool model. The two-pool model offers a compromise between the simple and more complex model, as it captures a thermally stable pool, which turns over 49% slower than the more reactive pool and 40% slower than the one-pool model (Table S6). Expanding ecosystem evolution models to include different turnover rates of fine SOC pools has the potential to improve predictions of marsh persistence, in the absence of disturbances.

4.3. Disturbances Alter SOC Reactivity

Decades following emergent grass dieback and submergence led to pond surface soils with different characteristics than the adjacent marsh. Collapse of marsh grass roots and water infilling of pore spaces contributed to higher water content, lower bulk densities, and initial subsidence (Figure 1, Chambers et al., 2019). Pond surface soils characterized with $F^{14}C$ < 1 and $\delta^{13}C$ values similar to marsh soils at the same elevation (1.17 m; Figures 3b and 3f) are consistent with limited accumulation of recent production from submerged plant and algal communities and imply that ponds do not trap exported detritus (Figure 3; Spivak et al., 2017). Moreover, the convergence in marsh and pond SOC reactivity at depth (<1 m NAVD88) (Figure 2) supports our comparative approach.

Over time, decomposition becomes an increasingly important mechanism driving pond deepening, as microbes assimilate buried peat and high respiration accounts for SOC loss (Spivak et al., 2017, 2018, 2020). Oxic surface waters during the day and benthic microalgal exudates may prime degradation of older, complex macromolecules (Fontaine et al., 2007; Spivak et al., 2017). Conditions favoring decomposition are confined to surface horizons due to limited gas diffusion and inhibition of bioturbating fauna by nighttime hypoxia (Spivak et al., 2017). Accordingly, *Ea* was greater in pond surface horizons than in deeper layers, and compared to the marsh at similar elevations (Figure 2i), but converged at depth (<1 m NAVD88) with the surrounding marsh. Progressive δ^{13}C-CO_2 enrichment with depth suggests that microbial reworking still occurs under less favorable, waterlogged conditions, but with limited effects on thermal reactivity (Figures 1a, 2h, 2i, and 3f–3i). Disturbances leading to pond formation therefore facilitated loss and shifts toward lower thermal reactivity of surface SOC, which could potentially slow progressive deepening.

5. Conclusions

We identified at least five geochemically distinct fine SOC pools (Figure 3), suggesting that slow-cycling marsh organic matter is more complex than typically conceptualized. By modeling downcore changes in fine SOC against soil geochronometers, we generated some of the first empirical estimates of turnover times (Figure 4). Carbon reactivity, source, and age described multiple processes contributing to soil development: new production, erosion and redeposition, and microbial reworking. Long-term decomposition and disturbances that accelerate decomposition (e.g., ponding) result in an accumulation of SOC with lower thermal reactivity. Further characterization of molecular composition within abiotic (e.g., redox) and biotic (e.g., microbial communities and carbon use efficiency) contexts may improve understanding of controls on decomposition and spatial variability in marsh SOC storage (Spivak et al., 2019). Broader application of these geochemical approaches has potential to enhance understanding of preservation under different environmental settings and inform marsh ecosystem evolution models and service valuation.

Data Availability Statement

Data are archived at BCO-DMO.org (Spivak, 2020a, 2020b, 2020c, 2020d) and sciencebase.gov (Luk et al., 2020).

References

Adamowicz, S. C., & Roman, C. T. (2005). New England salt marsh pools: A quantitative analysis of geomorphic and geographic features. *Wetlands*, *25*(2), 279.

Appleby, P. G., & Oldfield, F. (1978). The calculation of lead-210 dates assuming a constant rate of supply of unsupported ^{210}Pb to the sediment. *Catena*, *5*(1), 1–8. https://doi.org/10.1016/S0341-8162(78)80002-2

Barbier, E. B., Hacker, S. D., Kennedy, C., Koch, E. W., Stier, A. C., & Silliman, B. R. (2011). The value of estuarine and coastal ecosystem services. *Ecological Monographs*, *81*(2), 169–193. https://doi.org/10.1890/10-1510.1

Benner, R., Fogel, M. L., Sprague, E. K., & Hodson, R. E. (1987). Depletion of C in lignin and its implications for stable carbon isotope studies. *Nature*, *329*(6141), 708. https://doi.org/10.1038/329708a0

Bruun, S., Ågren, G. I., Christensen, B. T., & Jensen, L. S. (2010). Measuring and modeling continuous quality distributions of soil organic matter. *Biogeosciences*, *7*(1), 27–41. https://doi.org/10.5194/bg-7-27-2010

Bulseco, A. N., Giblin, A. E., Tucker, J., Murphy, A. E., Sanderman, J., Hiller-Bittrolff, K., &(2019). Nitrate addition stimulates microbial decomposition of organic matter in salt marsh sediments. *Global Change Biology*, *25*(10), 3224–3241. https://doi.org/10.1111/gcb.14726

Bulseco, A. N., Vineis, J. H., Murphy, A. E., Spivak, A. C., Giblin, A. E., Tucker, J., &(2020). Metagenomics coupled with biogeochemical rates measurements provide evidence that nitrate addition stimulates respiration in salt marsh sediments. *Limnology & Oceanography*, *65*, S321–S339. https://doi.org/10.1002/lno.11326

Chambers, L. G., Steinmuller, H. E., & Breithaupt, J. L. (2019). Toward a mechanistic understanding of "peat collapse" and its potential contribution to coastal wetland loss. *Ecology*, *100*(7), 1–15. https://doi.org/10.1002/ecy.2720

Cristina, R. A., Flores, J. B., Cardenas, V., Salazar, S. O. R., & Cervantes, L. D. (2018). *Bacillus amyloliquefaciens* as a plant growth promoting bacteria with the interaction with of grass salt *Distichlis palmeri* (Vasey) under field conditions, in desert of Sonora, Mexico. *Journal of Plant Science and Phytopathology*, *2*, 59–67. https://doi.org/10.29328/journal.jpsp.1001021

Day, J. W., Rybczyk, J., Scarton, F., Rismondo, A., Are, D., & Cecconi, G. (1999). Soil accretionary dynamics, sea-level rise and the survival of wetlands in Venice Lagoon: A field and modeling approach. *Estuarine, Coastal and Shelf Science*, *49*(5), 607–628. https://doi.org/10.1006/ecss.1999.0522

Engelhart, S. E., Horton, B. P., Douglas, B. C., Peltier, W. R., & Törnqvist, T. E. (2009). Spatial variability of late Holocene and 20th century sea-level rise along the Atlantic coast of the United States. *Geology*, *37*(12), 1115–1118. https://doi.org/10.1130/G30360A.1

Fontaine, S., Barot, S., Barré, P., Bdioui, N., Mary, B., & Rumpel, C. (2007). Stability of organic carbon in deep soil layers controlled by fresh carbon supply. *Nature*, *450*(7167), 277–280. https://doi.org/10.1038/nature06275

Gleixner, G., Poirier, N., Bol, R., & Balesdent, J. (2002). Molecular dynamics of organic matter in a cultivated soil. *Organic Geochemistry*, *33*(3), 357–366. https://doi.org/10.1016/S0146-6380(01)00166-8

Gonneea, M. E., Maio, C. V., Kroeger, K. D., Hawkes, A. D., Mora, J., Sullivan, R., et al. (2019). Salt marsh ecosystem restructuring enhances elevation resilience and carbon storage during accelerating relative sea-level rise. *Estuarine, Coastal and Shelf Science*, *217*, 56–68. https://doi.org/10.1016/j.ecss.2018.11.003

Haddad, R. I., & Martens, C. S. (1987). Biogeochemical cycling in an organic-rich coastal marine basin: 9. Sources and accumulation rates of vascular plant-derived organic material. *Geochimica et Cosmochimica Acta*, *51*(11), 2991–3001. https://doi.org/10.1016/0016-7037(87)90372-3

Hemingway, J. D., Galy, V. V., Gagnon, A. R., Grant, K. E., Rosengard, S. Z., Soulet, G., et al. (2017). Assessing the blank carbon contribution, isotope mass balance, and kinetic isotope fractionation of the ramped pyrolysis/oxidation instrument at nosams. *Radiocarbon*, *59*(1), 179–193. https://doi.org/10.1017/RDC.2017.3

Hemingway, J. D., Rothman, D. H., Rosengard, S. Z., & Galy, V. V. (2017). Technical note: An inverse method to relate organic carbon reactivity to isotope composition from serial oxidation. *Biogeosciences*, *14*(22), 5099–5114. https://doi.org/10.5194/bg-14-5099-2017

Hemminga, M. A., Kok, C. J., & De Munck, W. (1988). Decomposition of *Spartina anglica* roots and rhizomes in a salt marsh of the Westerschelde Estuary. *Marine Ecology Progress Series*, *48*, 175–184.

Hopkinson, C. S., Morris, J. T., Fagherazzi, S., Wollheim, W. M., & Raymond, P. A. (2018). Lateral marsh edge erosion as a source of sediments for vertical marsh accretion. *Journal of Geophysical Research: Biogeosciences*, *123*, 2444–2465. https://doi.org/10.1029/2017JG004358

Hughes, Z. J., FitzGerald, D. M., Wilson, C. A., Pennings, S. C., Wiçski, K., & Mahadevan, A. (2009). Rapid headward erosion of marsh creeks in response to relative sea level rise. *Geophysical Research Letters*, *36*, L03602. https://doi.org/10.1029/2008GL036000

Janik, L. J., Skjemstad, J. O., Shepherd, K. D., & Spouncer, L. R. (2007). The prediction of soil carbon fractions using mid-infrared-partial least square analysis. *Australian Journal of Soil Research*, *45*(2), 73–81. https://doi.org/10.1071/SR06083

Johnston, M. E., Cavatorta, J. R., Hopkinson, C. S., & Valentine, V. (2003). Importance of metabolism in the development of salt marsh ponds. *The Biological Bulletin*, *205*(2), 248–249. https://doi.org/10.2307/1543278

Kirwan, M. L., & Mudd, S. M. (2012). Response of salt-marsh carbon accumulation to climate change. *Nature*, *489*, 550–553. https://doi.org/10.1038/nature11440

Kirwan, M. L., & Murray, A. B. (2007). A coupled geomorphic and ecological model of tidal marsh evolution. *Proceedings of the National Academy of Sciences of the United States of America*, *104*(15), 6118–6122. https://doi.org/10.1073/pnas.0700958104

Kirwan, M. L., Murray, A. B., Donnelly, J. P., & Corbett, D. R. (2011). Rapid wetland expansion during European settlement and its implication for marsh survival under modern sediment delivery rates. *Geology*, *39*(5), 507–510.

Lehmann, J., Hansel, C. M., Kaiser, C., Kleber, M., Maher, K., Manzoni, S., et al. (2020). Persistence of soil organic carbon caused by functional complexity. *Nature Geoscience*, *13*, 529–534. https://doi.org/10.1038/s41561-020-0612-3

Luk, S. Y., Spivak, A. C., Eagle, M. J., & O'Keefe-Suttles, J. A. (2020). *Collection, analysis, and age-dating of sediment cores from a salt marsh platform and ponds in, Rowley, Massachusetts, in 2014–15: U.S. Geological Survey data release.* https://doi.org/10.5066/P9HIOWKT

Manzoni, S., Katul, G. G., & Porporato, A. (2009). Analysis of soil carbon transit times and age distributions using network theories. *Journal of Geophysical Research*, *114*, G04025. https://doi.org/10.1029/2009JG001070

Marín-Spiotta, E., Gruley, K. E., Crawford, J., Atkinson, E. E., Miesel, J. R., Greene, S., et al. (2014). Paradigm shifts in soil organic matter research affect interpretations of aquatic carbon cycling: Transcending disciplinary and ecosystem boundaries. *Biogeochemistry*, *117*(2–3), 279–297. https://doi.org/10.1007/s10533-013-9949-7

Mariotti, G., Spivak, A. C., Luk, S. Y., Ceccherini, G., Tyrrell, M., & Gonneea, M. E. (2020). Modeling the spatial dynamics of marsh ponds in New England salt marshes. *Geomorphology*, *365*, 107262. https://doi.org/10.1016/j.geomorph.2020.107262

McNichol, A. P., Osborne, E. A., Gagnon, A. R., Fry, B., & Jones, G. A. (1994). TIC, TOC, DIC, DOC, PIC, POC—Unique aspects in the preparation of oceanographic samples for ^{14}C-AMS. *Nuclear Instruments and Methods in Physics Research Section B: Beam Interactions with Materials and Atoms*, *92*(1–4), 162–165. https://doi.org/10.1016/0168-583X(94)95998-6

Morris, J. T., Barber, D. C., Callaway, J. C., Chambers, R., Hagen, S. C., Hopkinson, C. S., et al. (2016). Contributions of organic and inorganic matter to sediment volume and accretion in tidal wetlands at steady state. *Earth's Future*, *4*, 110–121. https://doi.org/10.1002/2015EF000334

Morris, J. T., & Bowden, W. B. (1986). A mechanistic, numerical model of sedimentation, mineralization, and decomposition for marsh sediments. *Soil Science Society of America Journal*, *50*(1), 96–105. https://doi.org/10.2136/sssaj1986.03615995005000010019x

Morris, J. T., Sundareshwar, P. V., Nietch, C. T., Kjerfve, B., & Cahoon, D. R. (2002). Responses of coastal wetlands to rising sea level. *Ecology*, *83*(10), 2869–2877. https://doi.org/10.1890/0012-9658(2002)083[2869:ROCWTR]2.0.CO;2

Ortiz, A. C., Roy, S., & Edmonds, D. A. (2017). Land loss by pond expansion on the Mississippi river delta plain. *Geophysical Research Letters*, *44*, 3635–3642. https://doi.org/10.1002/2017GL073079

Ouyang, X., & Lee, S. Y. (2014). Updated estimates of carbon accumulation rates in coastal marsh sediments. *Biogeosciences*, *11*(18), 5057–5071. https://doi.org/10.5194/bg-11-5057-2014

Peltier, W. R., Argus, D. F., & Drummond, R. (2015). Space geodesy constrains ice age terminal deglaciation: The global ICE-6G_C (VM5a) model. *Journal of Geophysical Research: Solid Earth*, *120*, 450–487. https://doi.org/10.1002/2014JB011176

Pendleton, L., Donato, D. C., Murray, B. C., Crooks, S., Jenkins, W. A., Sifleet, S., et al. (2012). Estimating global "blue carbon" emissions from conversion and degradation of vegetated coastal ecosystems. *PLoS One*, *7*(9), e43542. https://doi.org/10.1371/journal.pone.0043542

Pennington, W., Cambray, R. S., Eakins, J. D., & Harkness, D. D. (1976). Radionuclide dating of the recent sediments of Blelham Tarn. *Freshwater Biology*, *6*(4), 317–331. https://doi.org/10.1111/j.1365-2427.1976.tb01617.x

Redfield, A. C. (1972). Development of a New England salt marsh. *Ecological Monographs*, *42*(2), 201–237.

Reimer, P. J., Brown, T. A., & Reimer, R. W. (2004). Discussion: Reporting and calibration of post-bomb ^{14}C data. *Radiocarbon*, *46*(3), 1299–1304. https://doi.org/10.1017/S0033822200033154

Rosenheim, B. E., Day, M. B., Domack, E., Schrum, H., Benthien, A., & Hayes, J. M. (2008). Antarctic sediment chronology by programmed-temperature pyrolysis: Methodology and data treatment. *Geochemistry, Geophysics, Geosystems*, *9*, Q04005. https://doi.org/10.1029/2007GC001816

Sanderman, J., & Stuart Grandy, A. (2020). Ramped thermal analysis for isolating biologically meaningful soil organic matter fractions with distinct residence times. *Soils*, *6*(1), 131–144. https://doi.org/10.5194/soil-6-131-2020

Schile, L. M., Callaway, J. C., Morris, J. T., Stralberg, D., Parker, V. T., & Kelly, M. (2014). Modeling tidal marsh distribution with sea-level rise: Evaluating the role of vegetation, sediment, and upland habitat in marsh resiliency. *PLoS One*, *9*(2), e88760. https://doi.org/10.1371/journal.pone.0088760

Sollins, P., Swanston, C., Kleber, M., Filley, T., Kramer, M., Crow, S., et al. (2006). Organic C and N stabilization in a forest soil: Evidence from sequential density fractionation. *Soil Biology and Biochemistry*, *38*(11), 3313–3324. https://doi.org/10.1016/j.soilbio.2006.04.014

Spivak, A. C. (2020a). *Bulk soil and elemental properties of marsh and infilled pond soils collected in 2014–2015 within Plum Island Ecosystems LTER*. Biological and Chemical Oceanography Data Management Office (BCO-DMO). https://doi.org/10.26008/1912/bco-dmo.827298.1

Spivak, A. C. (2020b). *Fourier transform infrared spectroscopy raw spectra of soils collected in 2014–2015 within Plum Island ecosystems LTER*. Biological and Chemical Oceanography Data Management Office (BCO-DMO). https://doi.org/10.26008/1912/bco-dmo.827452.1

Spivak, A. C. (2020c). *Ramped pyrolysis oxidation (RPO) temperature and carbon dioxide evolved values of soils collected in 2014–2015 within Plum Island Ecosystems LTER*. Biological and Chemical Oceanography Data Management Office (BCO-DMO). https://doi.org/10.26008/1912/bco-dmo.827427.1

Spivak, A. C. (2020d). *Ramped pyrolysis oxidation (RPO) C isotope values of soils collected in 2014–2015 within Plum Island Ecosystems LTER*. Biological and Chemical Oceanography Data Management Office (BCO-DMO). https://doi.org/10.26008/1912/bco-dmo.827365.1

Spivak, A. C., Denmark, A., Gosselin, K. M., & Sylva, S. P. (2020). Salt marsh pond biogeochemistry changes hourly-to-yearly but does not scale with dimensions or geospatial position. *Journal of Geophysical Research: Biogeosciences*, *125*, e2020JG005664. https://doi.org/10.1029/2020JG005664

Spivak, A. C., Gosselin, K., Howard, E., Mariotti, G., Forbrich, I., Stanley, R., &(2017). Shallow ponds are heterogeneous habitats within a temperate salt marsh ecosystem. *Journal of Geophysical Research: Biogeosciences*, *122*, 1371–1384. https://doi.org/10.1002/2017JG003780

Spivak, A. C., Gosselin, K. M., & Sylva, S. P. (2018). Shallow ponds are biogeochemically distinct habitats in salt marsh ecosystems. *Limnology & Oceanography*, *63*(4), 1622–1642. https://doi.org/10.1002/lno.10797

Spivak, A. C., & Ossolinski, J. (2016). Limited effects of nutrient enrichment on bacterial carbon sources in salt marsh tidal creek sediments. *Marine Ecology Progress Series*, *544*, 107–130. https://doi.org/10.3354/meps11587

Spivak, A. C., Sanderman, J., Bowen, J. L., Canuel, E. A., & Hopkinson, C. S. (2019). Global-change controls on soil-carbon accumulation and loss in coastal vegetated ecosystems. *Nature Geoscience*, *12*(9), 685–692. https://doi.org/10.1038/s41561-019-0435-2

Trumbore, S. E. (1997). Potential responses of soil organic carbon to global environmental change. *Proceedings of the National Academy of Sciences of the United States of America*, *94*(16), 8284–8291. https://doi.org/10.1073/pnas.94.16.8284

Trumbore, S. (2009). Radiocarbon and soil carbon dynamics. *Annual Review of Earth and Planetary Sciences*, *37*(1), 47–66. https://doi.org/10.1146/annurev.earth.36.031207.124300

Watson, E. B., Wigand, C., Davey, E. W., Andrews, H. M., Bishop, J., & Raposa, K. B. (2017). Wetland loss patterns and inundation-productivity relationships prognosticate widespread salt marsh loss for southern New England. *Estuaries and Coasts*, *40*, 662–681. https://doi.org/10.1007/s12237-016-0069-1

Weston, N. B. (2014). Declining sediments and rising seas: An unfortunate convergence for tidal wetlands. *Estuaries and Coasts*, *37*(1), 1–23. https://doi.org/10.1007/s12237-013-9654-8

Williams, E. K., & Rosenheim, B. E. (2015). What happens to soil organic carbon as coastal marsh ecosystems change in response to increasing salinity? An exploration using ramped pyrolysis. *Geochemistry, Geophysics, Geosystems*, *16*, 2322–2335. https://doi.org/10.1002/2015GC005839

Wilson, J. O., Buchsbaum, R., Valiela, I., & Swain, T. (1986). Decomposition in salt marsh ecosystems: Phenolic dynamics during decay of litter of *Spartina alterniflora*. *Marine Ecology Progress Series*, *29*(2), 177–187. https://doi.org/10.3354/meps029177